



Small Scale Effect on Vibration of Thermally Postbuckled Monolayer Graphene Nanoribbon Based on Nonlocal Elasticity Theory

G.A. Varzandian¹, S. Ziaee*¹, M. Farid², A. Niknejad¹

¹ Department of Mechanical Engineering, Yasouj University, Yasouj, Iran.

² School of Mechanical Engineering, Shiraz University, Shiraz, Iran.

ABSTRACT: In the present research, vibration behavior is presented for a thermally postbuckled two side clamped monolayer graphene nanoribbon. The monolayer graphene nanoribbon is modeled as a nonlocal orthotropic plate strip which contains small scale effects. The formulations are based on the Kirchhoff's plate theory, and von Karman-type nonlinearity is considered in strain-displacement relations. The thermal effects are also included and the material properties are assumed to be temperature-dependent. The initial deflection caused by thermal postbuckling and internal loads are taken into account. A coupled system of equations is derived and a new semi analytical solution is obtained. The effects of variation of small scale parameter $e_0 a$ to the natural frequencies, deflections and mode shapes of graphene nanoribbon are analyzed and the numerical results are obtained from the nonlocal plate model; also, molecular dynamics simulations are used to investigate different properties of graphene nanoribbon including both buckling and vibrational behaviors. The small scale coefficient is calibrated using molecular dynamics simulations. Numerical results are compared with those of similar researches. Effects of various parameters on the postbuckled vibration of graphene nanoribbon in thermal environments such as scale parameter, length and thermal load are presented. Stability and occurrence probability of internal resonance between vibration modes around a buckled configuration is investigated.

Review History:

Received: 20 Mar. 2019

Revised: 24 May. 2019

Accepted: 16 Jun. 2019

Available Online: 23 Jun 2019

Keywords:

Graphene nanoribbon

Thermal postbuckling

Nonlocal plate model

Postbuckled vibration

Plate strip.

1. Introduction

Graphene is a 2 Dimensional (2-D) leaf that consists of carbon atoms in a hexagonal configuration. In a monolayer graphene sheet, each carbon atom connects to three other carbons. These bonds are in a single flat plate and all of them have the equal angles. Graphene structures have superior properties and they are introduced as one of the fundamental carbon forms and graphene is the base of many other configurations such as graphite, carbon nanotubes and fullerenes [1]; therefore, studying Single Layer Graphene Sheets (SLGSs) is very important in nanoscale studies [2]. Recently nanoscale structures such as nanobeams, nanoplates and the strip type of nanoplates that are called nanoribbons have gained considerable attention from both the experimental and theoretical researchers [3-7]. This is because nanostructures possess much superior mechanical, electrical, electronic, and thermal properties as compared to the conventional structural materials [8-10].

In nano scale plate problems, solutions due to classical theories such as Kirchhoff's plate theory and shear deformation plate theory usually have remarkable errors because in these theories, the relation between stress and strain is point wise and the size effects are not considered

[11]. In nonlocal elasticity theory, the stress at a reference point is assumed to be a functional of the strain field at every point in the body and the effects of scale are considered by a new quantity called scale parameter [12].

Based on Eringen's nonlocal elasticity theory, effects of size are taken into account by employing a scale parameter and applying it into classical continuum models [11,12]. Pradhan and Phadikar [13] used the nonlocal differential constitutive relations of Eringen to reformulation of CLassical Plate Theory (CLPT) and First-order Shear Deformation Theory (FSDT) of plates. Nazemnezhad [14] studied shear effect of Van Der Waals (VDWs) interactions on free vibration of a Multi-Layer Graphene NanoRibbon (MLG NR) in a cantilever form by employing nonlocal Timoshenko beam model and Molecular Dynamics (MD) simulations. He showed that the quantity of nonlocal parameter is directly related to the number of MLG NR layers, and its value increases by increasing the number of Graphene NanoRibbon (G NR) layers. Shi et al. [15] showed that the natural frequencies of MLG NR embedded in an elastic matrix are significantly influenced by nonlocal effects. Varzandian and Ziaee [7] proposed an analytical method for solution of non-linear free vibration of thin rectangular nanoplates with various boundary conditions based on non-local theory using Jacobi elliptic functions.

Nowadays MD simulations are widely used for modeling

*Corresponding author's email: ziaee@yu.ac.ir



the mechanical and thermal properties of nanoscale materials [14, 16-18]. Sen et al. [3] combined molecular dynamics and experimental data to studying the tearing of graphene sheets from adhesive substrates. Their research was also including the observation of the formation of tapered graphene nanoribbons. It has shown that tearing of graphene sheets leads to tapered nanoribbons by means of experimental studies and atomistic simulations [19]. Scarpa et al. [4] used an equivalent atomistic continuum Finite Element (FE) model and a molecular mechanics model based on the Universal Force Field (UFF) potential to simulation of the mechanical vibration, natural frequencies and acoustic wave dispersion characteristics of graphene nanoribbons.

Thermal effect has one of the most important roles on the vibration behaviors of structures in macro and also nano scales such as nanotubes and nanoplates. If the temperature of the plate is raised or lowered it expands or contracts, respectively. Within a certain temperature change, such expansion or contraction, for most structural materials, is directly proportional to the change in temperature. When a free plate made of homogeneous isotropic material is heated uniformly, there appear normal strains but no thermal stresses [20]. But for the case of graphene, considering thermal effects is very important [21]. Researchers showed that the thermal effects on the mechanical behaviors of the carbon nanotubes are obvious [22]. Wang et al. [23] showed that the vibration properties can be tuned by the thermal effects and the influences on the vibration behaviors are usually different for different modes. Na and Kim [24] investigated three-dimensional thermal buckling and postbuckling analyses of Functionally Graded (FG) materials subjected to uniform or non-uniform temperature rise for fully clamped plates by using finite element method. Nonlinear vibration behavior of a simply supported, single and bilayer graphene sheet in thermal environments is analyzed by Shen et al. [25,26].

Investigation of vibration around a buckled configuration at large scale is reported in some researches. Yamaki and Chiba [27] proposed theoretical analyses for nonlinear vibrations of a clamped rectangular plate with the effects of both initial deflection and initial edge displacement. The influence of initial deflections are also investigated for analysis of large deflection orthotropic plate under combined biaxial compression/tension and lateral pressure loads, considering the overall (grillage) buckling collapse mode [28]. Nayfeh and Emam [29] introduced an exact solution for stability and postbuckling configurations of beams with various boundary conditions. They showed that many internal resonances might be activated among the vibration modes around the same as well as different buckled configurations. In nano scale, there are many researches about buckling and vibrations separately and few of them are about vibration around a buckled configuration. Refaiejad et al [30] used a nonlocal higher order shear deformation beam theory to present an analytical solution for bending, buckling and vibration of FG nanobeams. An isogeometric vibration analysis of small-scale Timoshenko beams based on a novel size-dependent theory is investigated by taking

the nonlocal and strain gradient effects into account [31]. Nonlinear resonant behavior of microbeams over the buckled state is investigated by employing Hamilton's principle along with the modified couple stress theory [32]. In their research, the Galerkin scheme is used to discretize the nonlinear partial differential equation of motion into a set of ordinary differential equations. These sets of equations are solved numerically employing the pseudo-arclength continuation technique.

There are a large number of papers dealing with the analysis of buckling, postbuckling and vibration problems; however, to the authors' knowledge, there are few solutions for vibration analysis of buckled beams and buckled plates especially those due to thermal effects. Also, investigation of thermally buckled beam and plate vibration at large scale is noteworthy in some researches but is less seen for small scale such as nanobeams and nanoplates. So inquiries about dynamic behavior of nanoplates in various types and cases around a thermally buckled state are still open for research.

In the present research, a nonlocal plate strip model to study the vibration behavior of thermally postbuckled monolayer GNR is proposed. The governing equations are based on classical thin plate theory with a von Karman-type of nonlinearity and containing small scale effects. The thermal effects are also included and the material properties are assumed to be orthotropic and temperature-dependent. The stability analysis around the buckled configurations is considered. The effects of variation of small scale parameter

$e_0 a$ to the natural frequencies, deflections and mode shapes of GNR are analyzed, and the numerical results are obtained from the nonlocal plate model and some molecular dynamics simulations. The numerical illustrations show linear vibration response of Single Layer Graphene NanoRibbons (SLGNRs) under two side clamped and different sets of thermal, environmental and dimensional conditions.

It is also valuable to say that this research is useful for further investigating and analyzing the complex and nonlinear dynamics of postbuckled GNR in presence of internal resonance.

2. Theoretical Formulation

2.1. Deriving the primary equations of motion

A plate strip with length a and the Cartesian coordinate are considered for modeling the nanoribbon; also, the origin of the coordinate system is located in the middle of the strip as shown in Fig. 1.

Based on Eringen's [11,12] nonlocal elasticity theory, size effects are taken into account by the integration of a scale parameter into classical continuum models. In nonlocal elasticity theory, the stress at a reference is assumed to be a functional of the strain field point in the body. According to nonlocal elasticity theory, the nonlocal constitutive behavior of a Hookean solid is represented by the following differential equation [12]:

$$(1 - \mu^2 \nabla^2) \sigma^{nl} = \sigma^l \quad , \quad \mu = e_0 a \quad (1)$$

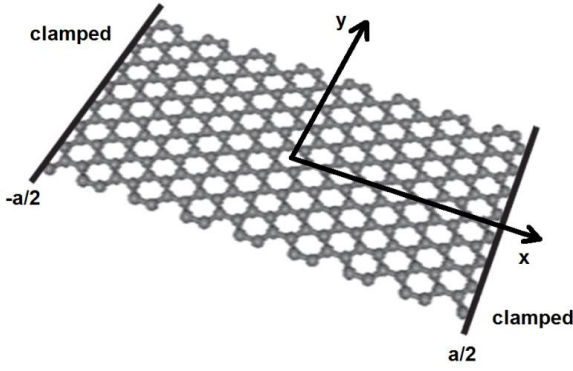


Fig. 1. Geometry of the nanoribbon

Here μ is the nonlocal parameter, σ^l is the local stress tensor and σ^d is the nonlocal stress tensor. Also ∇^2 is Laplacian operator in 2D Cartesian coordinate system.

Let U, W be components of the displacement vector of points in the middle surface of the plate occurring in the x and z directions, respectively. The displacement field for a postbuckled rectangular nanoplate is defined as following:

$$U = u + u_0 - z\partial(w + w_0)/\partial x, \quad W = w + w_0 \quad (2)$$

The capital letters represent the total displacements, small letters with the zero subscript introduces the displacement components of middle surface for postbuckled state (static problem) and small letters without subscript are for displacement components due to vibration.

Based on von Karman-type nonlinearity, the nonlinear strain components in the plate middle surface in postbuckled state are:

$$\begin{aligned} \epsilon_{xx}^0 &= \partial u / \partial x + \partial u_0 / \partial x + 1/2(\partial w / \partial x + \partial w_0 / \partial x)^2; \\ \epsilon_{yy}^0 &= 0; \quad \gamma_{xy}^0 = \partial(v + v_0) / \partial x \end{aligned} \quad (3)$$

The thermal forces N^T and moments M^T caused by elevated temperature are defined by [25]:

$$\begin{bmatrix} N_{xx}^T & M_{xx}^T \\ N_{yy}^T & M_{yy}^T \\ N_{xy}^T & M_{xy}^T \end{bmatrix} = \int_{-h/2}^{h/2} \begin{bmatrix} A_{xx}(T) \\ A_{yy}(T) \\ A_{xy}(T) \end{bmatrix} (1, z) \theta dz \quad (4)$$

And

$$\begin{bmatrix} A_{xx}(T) \\ A_{yy}(T) \\ A_{xy}(T) \end{bmatrix} = - \begin{bmatrix} \bar{E}_{11} & \bar{E}_{12} & \bar{E}_{13} \\ \bar{E}_{21} & \bar{E}_{22} & \bar{E}_{23} \\ \bar{E}_{31} & \bar{E}_{32} & \bar{E}_{33} \end{bmatrix} \begin{bmatrix} c^2 & s^2 \\ s^2 & c^2 \\ 2cs & -2cs \end{bmatrix} \begin{bmatrix} \alpha_1(T) \\ \alpha_2(T) \end{bmatrix} \quad (5)$$

In which \bar{E}_j are the transformed elastic constants, defined by [25]:

$$\begin{bmatrix} \bar{E}_{11} \\ \bar{E}_{12} \\ \bar{E}_{22} \\ \bar{E}_{13} \\ \bar{E}_{23} \\ \bar{E}_{33} \end{bmatrix} = \begin{bmatrix} c^4 & 2c^2s^2 & s^4 & 4c^2s^2 \\ c^2s^2 & c^4 + s^4 & c^2s^2 & -4c^2s^2 \\ s^4 & 2c^2s^2 & c^4 & 4c^2s^2 \\ c^3s & cs^3 - c^3s & -cs^3 & -2cs(c^2 - s^2) \\ cs^3 & c^3s - cs^3 & -c^3s & 2cs(c^2 - s^2) \\ c^2s^2 & -2c^2s^2 & c^2s^2 & (c^2 - s^2)^2 \end{bmatrix} \begin{bmatrix} E_{11} \\ E_{12} \\ E_{22} \\ E_{33} \end{bmatrix} \quad (6)$$

where $c = \cos \theta$, $s = \sin \theta$ and \bar{E}_j is the skew angle with respect to the plate x axis. Also, it is assumed that the effective Young's moduli E_j are temperature-dependent.

When $\theta = 0^\circ$, the type of graphene sheet is called armchair and for $\theta = 90^\circ$ its type is called zigzag.

The complete derivation of motion equations for 2D plates is accessible in the reference books [20,33]. For the plate strip case in which all derivatives with respect to y are equal to zero, by exerting material constants of graphene and nonlocal effects, the final equations of motion are simplified as following:

x-direction:

$$\begin{aligned} B_{11} \left\{ \frac{\partial^2 u}{\partial x^2} + \frac{\partial^2 u_0}{\partial x^2} + \frac{1}{2} \frac{\partial}{\partial x} \left(\frac{\partial w}{\partial x} + \frac{\partial w_0}{\partial x} \right) \right\} - \\ \frac{\partial N_{xx}^T}{\partial x} = \left(1 - \mu^2 \frac{\partial^2}{\partial x^2} \right) \left[I_0 \frac{\partial^2 u}{\partial t^2} \right] \end{aligned} \quad (7)$$

z-direction:

$$\begin{aligned} D_{11} \left(\frac{\partial^4 w}{\partial x^4} + \frac{\partial^4 w_0}{\partial x^4} \right) + \frac{\partial^2 M_{xx}^T}{\partial x^2} = \\ \left(1 - \mu^2 \frac{\partial^2}{\partial x^2} \right) \left(I_0 \left(\frac{\partial^2 u}{\partial t^2} \frac{\partial W}{\partial x} - \frac{\partial^2 W}{\partial t^2} \right) + \right. \\ \left. I_2 \left(\frac{\partial^4 W}{\partial x^2 \partial t^2} \right) + P + N_{xx} \frac{\partial^2 W}{\partial x^2} \right) \end{aligned} \quad (8)$$

where P is the lateral load and I_0, I_2 are mass moment of inertias and defined as:

$$(I_0, I_2) = \int_{-h/2}^{h/2} \rho (1, z^2) dz \quad (9)$$

2.2. Postbuckling equations

Using the linearized buckling analysis, only the initial elastic buckling of nanoplates and the critical forces and stresses can be found [20]. By considering the postbuckling analysis, a different behavior of nanoplate is revealed. The equilibrium configuration is divided into stable and unstable states and the critical points are observed which denoted the borders of two mentioned regions.

For mathematical analysis, a relation between compressive axial forces due to thermal loads and deflection must be calculated. This connection is usually in the form of parabolic function for a rectangular nanoplate and changes with variation of modes. Substituting time dependent terms

in primary equations of motion equal to zero and eliminating lateral load P yields:
x-direction:

$$B_{11} \left\{ \frac{\partial^2 u_0}{\partial x^2} + \frac{1}{2} \frac{\partial}{\partial x} \left(\frac{\partial w_0}{\partial x} \right)^2 \right\} - \frac{\partial N_{xx}^T}{\partial x} = 0 \quad (10)$$

z-direction:

$$D_{11} \left(\frac{\partial^4 w_0}{\partial x^4} \right) + \frac{\partial^2 M_{xx}^T}{\partial x^2} = \left(1 - \mu^2 \frac{\partial^2}{\partial x^2} \right) \left(N_{xx}^0 \frac{\partial^2 w_0}{\partial x^2} \right) \quad (11)$$

But from the equation of motion in x-direction and by considering $\partial/\partial y = 0$, $\partial/\partial t = 0$ it is observed that $\partial N_x^0 / \partial x = 0$ or $N_x^0 = K = cte$; So:

$$D_{11} \frac{\partial^4 w_0}{\partial x^4} = N_{xx}^0 \left(\frac{\partial^2 w_0}{\partial x^2} - \mu^2 \frac{\partial^4 w_0}{\partial x^4} \right) \quad (12)$$

And by considering plate strip case ($\partial/\partial y = 0$) yields

$$N_{xx}^0 - \mu^2 \frac{\partial^2 N_{xx}^0}{\partial x^2} = B_{11} \epsilon_{xx}^0 + C_{11} k_{xx} - N_{xx}^T \quad (13)$$

Then by supposing material properties reported in reference [25], the axial load N_x^0 is:

$$N_{xx}^0 = B_{11} \left(\frac{\partial u_0}{\partial x} + \frac{1}{2} \left(\frac{\partial w_0}{\partial x} \right)^2 \right) - N_{xx}^T \quad (14)$$

Hence, substituting Eq. (14) into Eq. (12) and simplification yields:

$$D_{11} \frac{\partial^4 w_0}{\partial x^4} - B_{11} \frac{\partial u_0}{\partial x} \frac{\partial^2 w_0}{\partial x^2} + \mu^2 B_{11} \frac{\partial u_0}{\partial x} \frac{\partial^4 w_0}{\partial x^4} - \frac{1}{2} B_{11} \frac{\partial^2 w_0}{\partial x^2} \left(\frac{\partial w_0}{\partial x} \right)^2 + \frac{1}{2} \mu^2 B_{11} \frac{\partial^4 w_0}{\partial x^4} \left(\frac{\partial w_0}{\partial x} \right)^2 + N_{xx}^T \frac{\partial^2 w_0}{\partial x^2} - \mu^2 N_{xx}^T \frac{\partial^4 w_0}{\partial x^4} = 0 \quad (15)$$

Investigating the applications of nanoribbons reveals that they are extensively used for very sensitive tools and refined sensors such as nano resonators and mass detectors that commonly are mounted in two sided fixed (or clamped) configuration [5, 34-35]; So, the solution of the problem is reported for this type of boundary condition. In this case, all boundary conditions are displacement boundary conditions and thus do not rely on the constitutive relations. The boundary conditions for a two side clamped plate strip are:

$$\begin{aligned} u_0(-a/2) &= u_0(a/2) = 0, \\ w_0(-a/2) &= w_0(a/2) = \\ \partial w_0(-a/2) / \partial x &= \partial w_0(a/2) / \partial x = 0 \end{aligned} \quad (16)$$

where a is the length of GNR and coordinate center is placed in the middle (Fig. 1). For seeking an approximate solution, variational or energy methods are usually used. Two well-known energy methods are Galerkin and Ritz [33]; Among these two methods, the Galerkin method is more general, because it doesn't need any quadratic functional nor virtual work principle [20]; Moreover, this method can be applied successfully to diverse types of problems of applied elasticity including the plate bending problems and so is used for the rest of the calculations.

One admissible form for satisfying the above boundary conditions is:

$$\begin{aligned} u_0(x) &= \sum_m u_{0m} \cos((2m-1)\pi x/a), \\ w_0(x) &= \sum_m w_{0m} \cos^2((2m-1)\pi x/a), \\ m &= 1, 2, \dots, j \end{aligned} \quad (17)$$

where j is the degree of freedom in both directions. Galerkin formulation is [33]:

$$\int_A \Gamma_N [u_i, \Psi_i^N(x)] \Psi_j^N(x) dx = 0, \quad i = 1, 2, \dots, N \quad (18)$$

Here $\Psi_i^N(x)$ are the admissible shape functions, u_i are components of displacement and is the left hand side of governing equations. Applying the Galerkin method to Eqs. (10) and (15) and Γ_N using Eq. (17) yields the long formulation system of nonlinear algebraic equations that reported in Appendix A.

Eq. (A1) is a system of $2j$ nonlinear equations with $2j$ unknown functions. Solving these equations, the displacement components are achieved. This system is solved by Newton method which is highly efficient for the solution of nonlinear algebraic equations. For getting the final results, initial guess is set to linear solution of the system equations and by repetition of the method, final solution is obtained.

2.3. Stability analysis

In this section, the dynamic stability of a buckled configuration is investigated. For this purpose, a small dynamic disturbance around the buckled configuration is considered. After calculations of displacements due to buckling state, the total components of displacements and natural frequency of nanoribbon are computable. By considering postbuckling solution, primary equation of motion in z-direction is simplified as following:

$$D_{11} \left(\frac{\partial^4 w}{\partial x^4} \right) + \left(1 - \mu^2 \frac{\partial^2}{\partial x^2} \right) \left[I_2 \left(\frac{\partial^4 w}{\partial x^2 \partial t^2} \right) - N_{xx} \frac{\partial^2 w}{\partial x^2} - \left(N_{xx} - N_{xx}^0 \right) \frac{\partial^2 w_0}{\partial x^2} \right] = 0 \quad (19)$$

Again by considering plate strip case ($\partial/\partial y = 0$) yields:

$$N_{xx} - \mu^2 \frac{\partial^2 N_{xx}}{\partial x^2} = B_{11} \left(\frac{\partial u}{\partial x} + \frac{\partial u_0}{\partial x} + \frac{1}{2} \left(\frac{\partial w}{\partial x} + \frac{\partial w_0}{\partial x} \right)^2 \right) - N_{xx}^T \quad (20)$$

Then using Eq. (14):

$$N_{xx} - N_{xx}^0 = B_{11} \left(\frac{\partial u}{\partial x} + \frac{1}{2} \left(\frac{\partial w}{\partial x} \right)^2 + \frac{\partial w_0}{\partial x} \frac{\partial w}{\partial x} \right) + \mu^2 \frac{\partial^2 N_{xx}}{\partial x^2} \quad (21)$$

But from equation of motion in x-direction and by differentiating yields:

$$\frac{\partial^2 N_{xx}}{\partial x^2} = I_0 \frac{\partial^3 u}{\partial x \partial t^2} \quad (22)$$

So

$$N_{xx} - N_{xx}^0 = B_{11} \left(\frac{\partial u}{\partial x} + \frac{1}{2} \left(\frac{\partial w}{\partial x} \right)^2 + \frac{\partial w_0}{\partial x} \frac{\partial w}{\partial x} \right) + \mu^2 I_0 \frac{\partial^3 u}{\partial x \partial t^2} \quad (23)$$

Substituting into Eq. (19) results in:

$$D_{11} \left(\frac{\partial^4 w}{\partial x^4} \right) + \left(1 - \mu^2 \frac{\partial^2}{\partial x^2} \right) \left[I_0 \frac{\partial^2 w}{\partial t^2} \frac{\partial (w + w_0)}{\partial x} \right] - \left[B_{11} \left(\frac{\partial u}{\partial x} + \frac{\partial u_0}{\partial x} + \frac{1}{2} \left(\frac{\partial w}{\partial x} + \frac{\partial w_0}{\partial x} \right)^2 \right) - N_{xx}^T + \mu^2 I_0 \frac{\partial^3 u}{\partial x \partial t^2} \right] \frac{\partial^2 w}{\partial x^2} - \left[B_{11} \left(\frac{\partial u}{\partial x} + \frac{1}{2} \left(\frac{\partial w}{\partial x} \right)^2 + \frac{\partial w_0}{\partial x} \frac{\partial w}{\partial x} \right) + \mu^2 I_0 \frac{\partial^3 u}{\partial x \partial t^2} \right] \frac{\partial^2 w_0}{\partial x^2} = 0 \quad (24)$$

For the case of linear vibration, by using material properties of a monolayer graphene sheet reported in reference [25], neglecting the nonlinear terms and after substitution and simplifications, the following equations are achieved in x and z-direction:

$$B_{11} \left\{ \frac{\partial^2 u}{\partial x^2} + \frac{\partial^2 w_0}{\partial x^2} \frac{\partial w}{\partial x} + \frac{\partial w_0}{\partial x} \frac{\partial^2 w}{\partial x^2} \right\} = \left(1 - \mu^2 \frac{\partial^2}{\partial x^2} \right) \left[I_0 \frac{\partial^2 u}{\partial t^2} \right], \quad \left[I_0 \left(\frac{\partial^2 w}{\partial t^2} - \frac{\partial w_0}{\partial x} \frac{\partial^2 u}{\partial t^2} \right) - I_2 \left(\frac{\partial^4 w}{\partial x^2 \partial t^2} \right) - \left(B_{11} \frac{\partial u_0}{\partial x} + \frac{1}{2} B_{11} \left(\frac{\partial w_0}{\partial x} \right)^2 \right) \frac{\partial^2 w}{\partial x^2} - N_{xx}^T \right] = 0 \quad (25)$$

$$D_{11} \left(\frac{\partial^4 w}{\partial x^4} \right) + \left(1 - \mu^2 \frac{\partial^2}{\partial x^2} \right) \left[\left(B_{11} \frac{\partial u_0}{\partial x} + \frac{1}{2} B_{11} \left(\frac{\partial w_0}{\partial x} \right)^2 \right) \frac{\partial^2 w}{\partial x^2} - N_{xx}^T \right] - \left[B_{11} \left(\frac{\partial u}{\partial x} + \frac{\partial w_0}{\partial x} \frac{\partial w}{\partial x} \right) + \mu^2 I_0 \frac{\partial^3 u}{\partial x \partial t^2} \right] \frac{\partial^2 w_0}{\partial x^2} = 0$$

Again applying the Galerkin method to Eq. (25) and supposing $u = u(x)e^{i\omega t}$, $w = w(x)e^{i\omega t}$ in which ω is the natural frequency where:

$$u(x) = \sum_m u_m \cos(\alpha x), \quad w(x) = \sum_m w_m \cos^2(\alpha x), \quad (26)$$

$$\alpha = (2m-1)\pi/a, \quad m = 1, 2, \dots$$

Yields the long formulation system of nonlinear algebraic equations that reported in Appendix B.

Eq. (B1) is a system of nonlinear equations with unknown functions. Solving this system of equations by Newton method, the displacement components due to vibration are achieved.

Eq. (B1) also represents an eigenvalue problem for ω . For a stable buckled configuration, ω^2 must be positive [29], and hence ω is real. To investigate the stability of the buckled shapes, according to reference [29] letting q_x^T be a little greater than critical buckling load (for example $q_x^T = 1.001q_{xcr}^T$) and exploring concerned physical mode shape, the stable and unstable positions are revealed.

3. Molecular Dynamics Simulation

One of the most famous numerical methods for analysis of nano structures is the molecular dynamics simulation. This method is relevant to the interaction between the atoms and molecules in a large system [36]. Employing this method is successful if the true and accurate potential function is selected.

In the present work, all simulations are performed using the molecular dynamics simulator ‘‘Lammps’’. Lammps is a free open source MD simulator which has suitable features that can be used to model different mechanical and thermal loading conditions of nanostructures. To modeling of two sides clamped boundary conditions, four layers of

carbon atoms should be fixed at two parallel sides of the graphene sheet [36]. To explain the long-range van der Waals interaction (Lenard Jones terms), the short-range covalent C–C interactions and torsion interactions, the Adaptive Intermolecular Reactive Empirical Bond Order (AIREBO) potential [37] is accomplished. AIREBO is a potential energy which is widely used to describe mechanical properties of carbon-based nanomaterials such as graphene and carbon nanotubes. For beginning the MD simulation, the nanoribbon is optimized initially and relaxed to reach the minimum energy configuration; also, the effective thickness $h=0.34\text{ nm}$ is used for analysis. After simulating the boundary conditions appropriately, the natural frequencies of SLGNR are calculated at different temperatures. Then, by adapting the results obtained from theoretical method and MD simulations, the small scale parameter is achieved at different thermal environmental conditions. Numerical quantities of e_0a for some temperatures and chirality conditions are reported in numerical section.

4. Verification

In this section, first of all, convergence for present approach is investigated; then, vibration behaviors of a postbuckled aluminum plate strip subjected to an axial load and with two clamped edges are analyzed.

To show the rate of convergence for present approach, the Galerkin results of critical buckling temperature for different scale parameters and some number of basic functions are listed in Table 1. The numerical results in Table 1 are obtained for orthotropic single-layered zigzag graphene nanoribbon. A fast rate of convergence of the present approach is evident for all values of scale parameters. Also, more investigation of the results reveals that 3 terms of basic functions are suited for using in calculations.

Although in present work only the thermal load is considered and physical axial load is not presented, but effect of the thermal load (N_x^T) is comparable with the axial load (N_x, N_x^0) with the aid of Eqs. (14) and (23). In both cases, these loads become apparent only in the in-plane load term of motion equation. Material properties used in verification process are represented in Table 2. Results are displayed in Table 3 and show that there is close agreement between the results of the present approach (for 3 terms of basic functions used for calculation) and those of separation of variables method [38].

For the rest of the calculations, a zigzag single layer

Table 2. Material properties of aluminum (Alloy 1100-H14, 99%A1) plate strip [38]

Properties	Value
Young's modulus (GPa)	70
Poisson's ratio	0.346
Density (kg/m^3)	2710

Table 3. First five frequencies of Al plate strip (rad/s)

	Ref.[38]	Present
λ_1	2761.706	2761.177
λ_2	10162.422	10161.978
λ_3	21560.441	21560.064
λ_4	36742.969	36742.278
λ_5	55862.672	55862.245

graphene nanoribbon with temperature dependent material properties is investigated. The numerical quantities of material properties are deduced from reference [25]. For further inspection of the method, the relation between the natural frequency and the scale coefficient is plotted in Fig. 2 for vibration around the first buckled configuration and compared to exact solution method suggested by reference [29]. Again 3 terms of basic functions are used for calculation.

Verification studies for MD simulations involving both buckling and vibrational studies are displayed in Fig. 3 and Table 4.

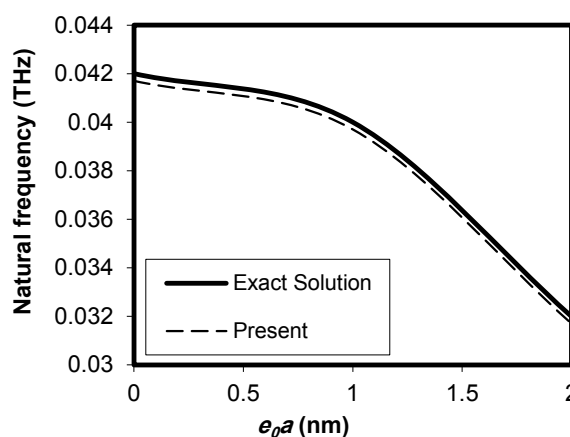


Fig. 2. Relation between the natural frequency and the scale coefficient with the high temperatures for mode I and $T = 700\text{ K}$.

Table 1. Convergence study for the Galerkin method.

Scale parameter (e_0a)	Number of basic functions used for calculation of critical buckling temperature				
	1	2	3	4	5
0.0	395.21	394.37	393.42	393.42	393.42
0.5	383.54	382.63	381.09	381.09	381.09
1.0	366.62	364.93	363.05	363.05	363.05
1.5	349.08	347.64	346.21	346.21	346.21
2.0	333.02	331.43	330.07	330.07	330.07

Table 4. Resonant frequencies of clamped zigzag single-layered graphene sheets.

MD (THz) Present study	MD (THz) reference [36]	Side length of square SLGS (nm)
0.1147461	0.1146223	10
0.0519233	0.0517078	15
0.0311567	0.0306219	20
0.0180037	0.0179975	25
0.0134090	0.0132953	30
0.0104284	0.0104182	35
0.0081272	0.0081090	40
0.0069476	0.0067681	45
0.0058614	0.0056362	50

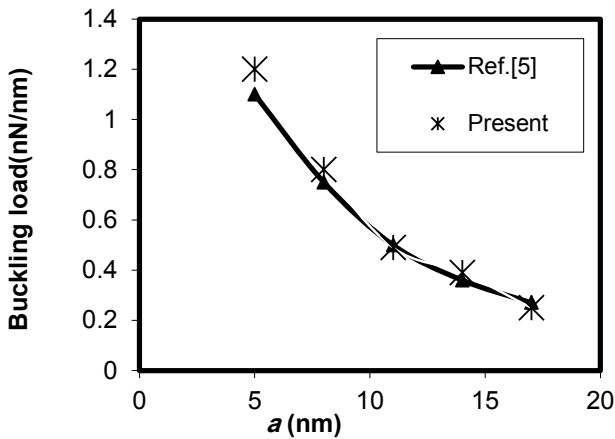


Fig. 3. Fundamental critical buckling load per width ratio of a Zigzag Graphene NanoRibbon (ZGNR) versus length for the fixed-fixed boundary conditions.

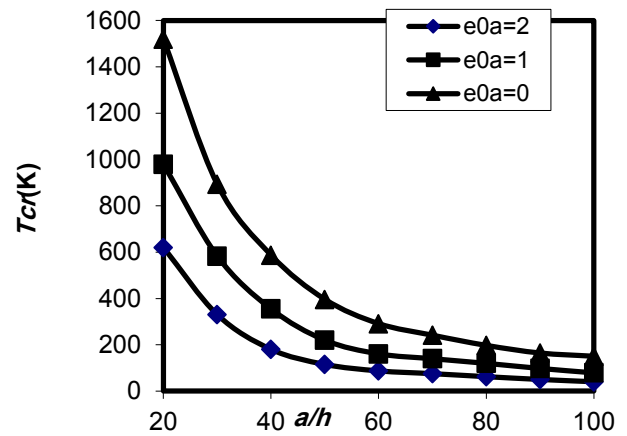


Fig. 4. Critical temperature gradient with respect to a/h under uniform temperature rise.

5. Numerical Results

5.1. Postbuckling results

After estimating the accuracy of the method, the numerical results are presented. The following material properties are used for the calculations:

$$E = 1 \text{TPa}, \nu = 0.3, \rho = 2250 \text{kg/m}^3, h = 0.34 \text{nm}, a = 10 \text{nm}$$

For determination of the critical temperature, the thermal buckling analysis is carried out. From Eq. (15), the thermal force N_x^T was computed explicitly with respect to the function of θ . Considering linear part of Eq. (15) and the related boundary conditions, the critical temperatures can be obtained by differentiating this equation and solving it numerically (Newton method). Fig. 4 gives the variation of the critical temperature gradient of clamped plate strip

under uniform temperature rise. Results show that critical temperature has reverse relation with scale parameter and as a result of employing the nonlocal theory, critical temperature is decreased.

After confirming the accuracy of the MD simulation in previous section, numerical studies are employed and results for postbuckling region are shown in the following:

The bifurcation diagram for the first three buckled configurations of a two side clamped GNR is plotted in Fig. 5, as the temperature is increased. As the thermal load exceeds the first critical buckling temperature, the nanoribbon loses stability and buckles. If the thermal load is increased beyond the second critical buckling temperature, nanoribbon has three positions: the one straight configuration and two buckled configurations. The stability of these positions is

Table 5. Critical buckling temperature of clamped zigzag single-layered graphene nanoribbon (K).

MD (K) Present study	Nonlocal continuum model (K) (The values of correspondent e_{0a} are in parenthesis.)	Side length of SLGNR (nm)
611.24	611.57 (1.934)	5
319.67	320.04 (0.598)	8
233.14	233.69 (0.201)	11
206.21	205.87 (0.147)	14
190.26	189.74 (0.101)	17

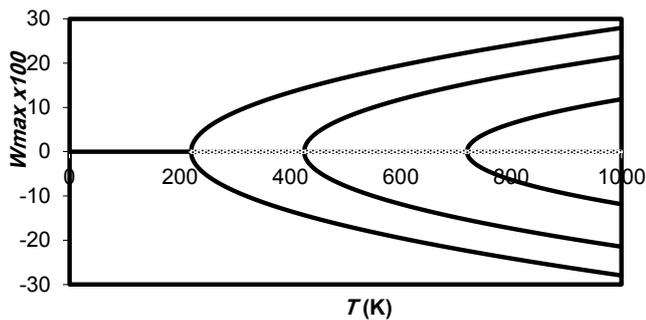


Fig. 5. Bifurcation diagram of the system with temperature rise.

determined in the next section.

Fig. 6 shows the comparison between the bifurcation diagrams of the system obtained via the nonlocal and the classical theories. It is seen that as a result of taking into account the scale parameter (i.e. employing the nonlocal theory), the beginning of bifurcation is transferred to a lower temperature and it shows the importance of employing the nonlocal theory in the modeling of nanoribbons.

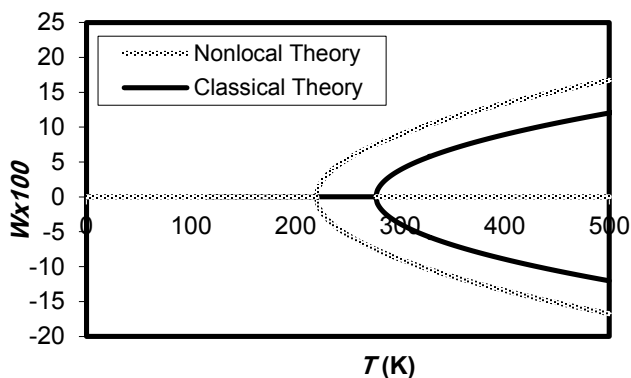


Fig. 6. Comparison between the bifurcation diagrams of the system obtained via nonlocal and classical theories for a zigzag GNR.

The numerical results for postbuckled zigzag GNR are given for different modes and nonlocal parameter (Fig. 7). In this figure the non-dimensional deflection of postbuckled clamped plates are depicted. It can be easily seen that increasing nonlocal parameter increases the non-dimensional deflection at the different points of the plate strip.

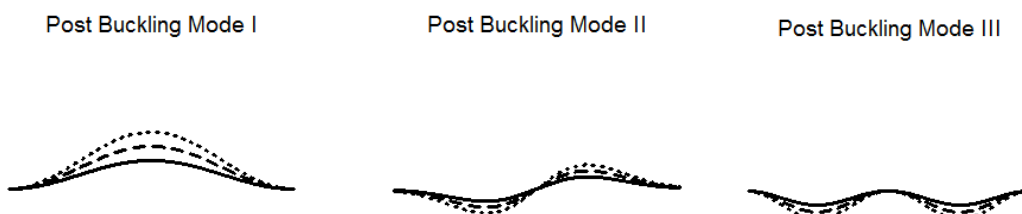


Fig. 7. Effects of nonlocal parameter on different mode shapes of postbuckled GNR, solid lines for $\mu = 0$, dashed lines for $\mu = 1$ and dotted lines for $\mu = 2$.

5.2. Stability and vibration results

After representing the accuracy of the formulation, a parametric study of the frequency for the linear vibration of thermally postbuckled monolayer GNR is presented.

For determining the stability, the method suggested in section 2.3 is used. Investigations showed that for the first buckled configuration, all of the positive roots of ω correspond to physical mode shapes. As a result, the first buckled configuration is a stable equilibrium position. However, further examinations showed that the upper modes of buckled configurations from mode II to V have unstable equilibrium position.

In continuation, a parametric study is carried out to show the effects of the nonlocal parameter in conjunction with the geometrical and material parameters on the vibration characteristics of the monolayer GNR.

In Fig. 8 the effects of scale parameter for instance on the first mode of plate vibration with increasing temperature is shown and indicates that without considering nonlocal effects, critical points and the solution are completely different.

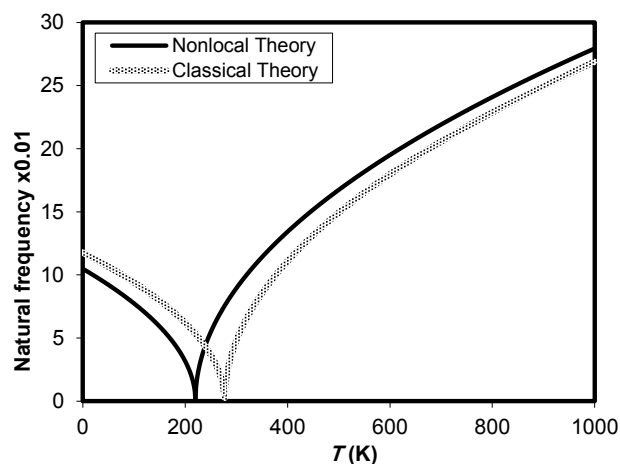


Fig. 8. Effects of nonlocal scale parameter in the evolution of natural frequency with increasing temperature before and after buckling of ZGNR for mode I.

In Figs. 9 to 11, variation of the vibration frequencies around the first three buckled configuration with the temperature is presented. Solid lines indicate odd vibration modes and dotted lines indicate even ones. This figure

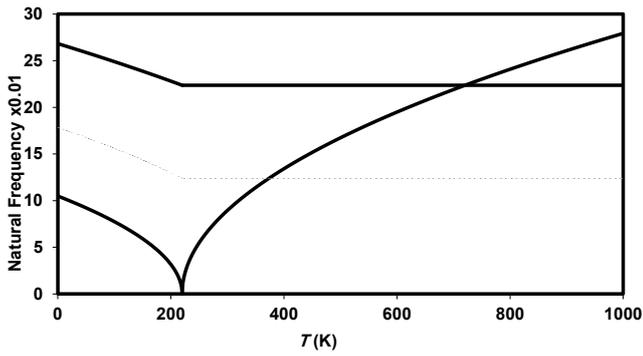


Fig. 9. Variation of the natural frequencies of vibration around the 1st buckled configuration of a two side clamped ZGNR

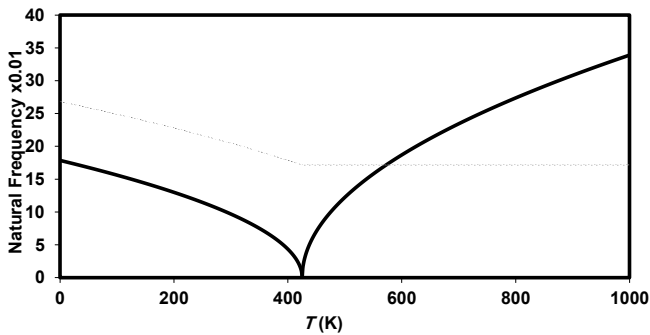


Fig. 10. Variation of the natural frequencies of vibration around the 2nd buckled configuration of a two side clamped ZGNR

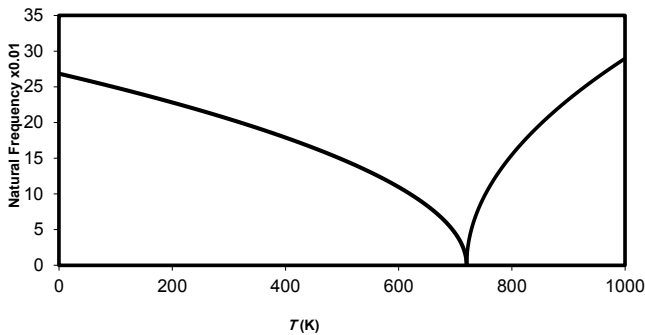


Fig. 11. Variation of the natural frequencies of vibration around the 3rd buckled configuration of a two side clamped ZGNR

shows that internal resonances, such as one-to-one, two-to-one, and three-to-one, might be activated between vibration modes around the buckled configuration. For example, a one-to-one internal resonance might be activated at $T=639K$, $978K$ around mode I, III respectively and also two-to-one at

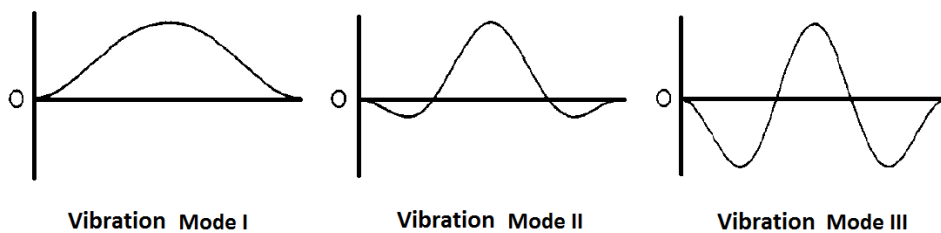


Fig. 12. Three first modes of vibration around the postbuckled state.

$T=456K$ around mode II. Also, further inspection indicates that a three-to-one internal resonance might be activated at $T=437K$ around mode II and also two-to-one at $T=779K$ around mode III.

The vibration modes around the first buckling mode of plate are shown in Fig. 12.

MD simulation results for frequency calculations are shown in Table 6 and Fig. 13.

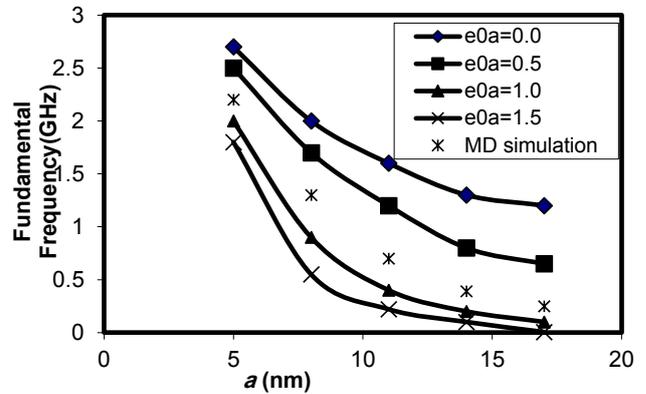


Fig. 13. Fundamental frequencies of clamped zigzag single-layered graphene nanoribbon

5.3. Chirality effects investigation

Fig. 14 shows the effects of temperature change on the vibration amplitude of the two types of postbuckled monolayer GNR for $a/h=50$. It can be seen that under the same thermal environmental condition and for the same aspect ratio, the armchair sheets will have lower natural

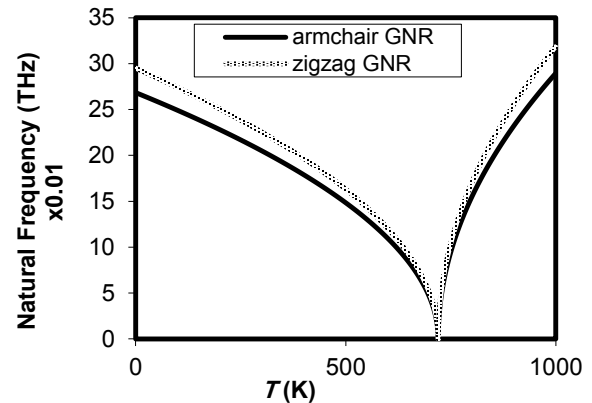


Fig. 14. Comparison between linear frequencies aroused from vibration around third buckling mode of an armchair and zigzag GNR under the same thermal environmental and dimensional condition ($a/h=50$)

Table 6. Resonant frequencies of clamped zigzag single-layered graphene nanoribbon.

MD (GHz)	Nonlocal continuum model (GHz)	Side length of SLGNR (nm)
Present study	(The values of correspondent e_0a are in parenthesis.)	
2.2239	2.2241 (1.934)	5
1.3142	1.3148 (0.598)	8
0.7438	0.7440 (0.201)	11
0.3912	0.3905 (0.147)	14
0.2565	0.2552 (0.101)	17

frequencies than those of zigzag sheets. This difference is due to different chirality and heteromorphic structure of two mentioned sheets.

More investigations on chirality effect are shown in Figs. 15 and 16. According to these figures, critical buckling temperature is negligibly influenced by chirality for a given graphene nanoribbon; also, results show that the chirality has an important influence on the natural frequencies at higher modes of vibration.

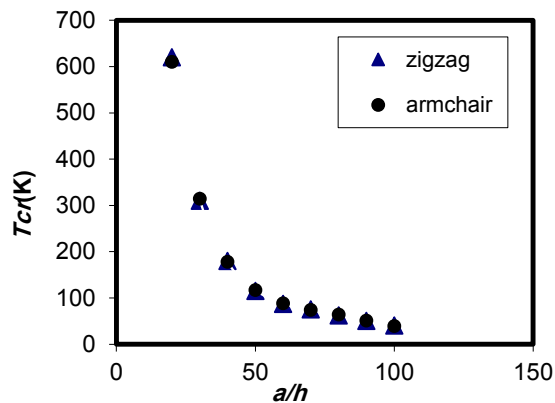


Fig. 15. Comparison between critical buckling temperatures for two cases of zigzag and armchair GNR

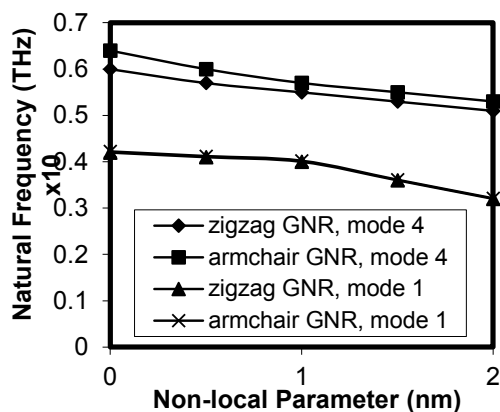


Fig. 16. Natural frequency of single-layered GNR with clamped edge and different chirality

6. Conclusion

In this research, vibration response of postbuckled monolayer graphene nanoribbon has been investigated on the basis of a nonlocal plate strip model and MD simulation for two side clamped boundary condition. The major difference between present model and previous ones in literature is that the present solution includes the deflection caused by

thermal postbuckling. Solution of the problem is posed into two phases, one is the thermally equilibrium phase (static problem) and another one is the small amplitude vibrations around the static response. In thermal postbuckling analysis, the bifurcation-type buckling behavior is observed and a thermal postbuckling equilibrium path is obtained. The complete formulation of nonlinear vibration of postbuckled GNR is presented and by neglecting the nonlinear terms, solution of linear vibration is introduced by solving a system of nonlinear algebraic equations. A stability analysis is also considered using an Eigen value problem in terms of frequency. By using MD simulations, some calibrated small scale coefficients are obtained for both vibration and postbuckling analysis. The effect of chirality on the buckling temperature, modes and vibration behavior of nanoribbon under similar thermal environmental and dimensional condition by considering two types of zigzag and armchair GNR is analyzed. The numerical results show that although the critical buckling temperature is negligibly influenced by chirality, its effect on vibration behavior is remarkable. Also results show that the armchair sheets will have lower natural frequencies than those of zigzag sheets when the two sheets have the same dimensional properties and thermal environmental condition; also, this effect is highlighted more on higher modes. The stability analysis reveals that the first buckling mode is a stable equilibrium position; whereas, buckled configurations beyond the first buckling mode are found to be unstable equilibrium positions. It also reveals that many internal resonances might be activated among vibration modes around the same buckled configuration for the case of fixed-fixed plate strip. Effect of scale parameter on the different quantities such as natural frequency, critical temperature and mode shapes is investigated. It is seen that as a result of employing the nonlocal theory, the beginning of bifurcation is transferred to a lower temperature; consequently, taking into account the length scale parameter decreases the flexural stiffness of the system and hence precipitates the onset of the bifurcation. Also, increasing nonlocal parameter increases the nondimensional deflection of the plate strip. By increasing temperature, the natural frequencies have two opposing behaviors; decreasing before buckling state and increasing after buckling state. Also considering scale parameter has two different effects, by increasing temperature before buckling, considering scale parameter decreases the natural frequency whereas in postbuckled state, it increases the natural frequency. The results shows that scale parameter and temperature change have a significant role on linear vibration of postbuckled nanostructures. These results also

open the door for further investigations into the complex and non-linear dynamics of postbuckled GNR.

Appendix A: Postbuckling equation

The algebraic equation arising from the Galerkin integration (Eq. (18)) for the postbuckling case is:

$$\begin{aligned}
 &60a \sum_m m^2 u_{0m} - 64 \sum_m m w_{0m} \sum_n n w_{0n} - 60a \sum_m m u_{0m} + 64 \sum_m m w_{0m}^2 + 15a \sum_m u_{0m} - 16 \sum_m w_{0m} \sum_n w_{0n} = 0, \\
 &-11520\pi^5 \mu^2 B_{11} \sum_m m^5 w_{0m}^2 + 14400\pi^5 \mu^2 B_{11} \sum_m m^2 w_{0m} \sum_n n^2 w_{0n} - 9600\pi^5 \mu^2 B_{11} \sum_m m^3 w_{0m}^2 + \\
 &3600\pi^5 \mu^2 B_{11} \sum_m m w_{0m} \sum_n n w_{0n} + 3840\pi^5 \mu^2 B_{11} \sum_m m^3 w_{0m} \sum_n n^3 w_{0n} - 720\pi^5 \mu^2 B_{11} \sum_m m w_{0m}^2 + \\
 &360\pi^3 a^2 B_{11} \sum_m m w_{0m} \sum_n n w_{0n} - 120\pi^3 a^2 B_{11} \sum_m m w_{0m}^2 - 11520\pi^3 a^2 \mu^2 N_{xx}^T \sum_m m \sum_n n + 3840\pi^3 a^2 \mu^2 N_{xx}^T \sum_m m - \\
 &7680\pi^3 a^2 \mu^2 N_{xx}^T \sum_m m^2 \sum_n n^2 + 15360\pi^3 a^2 \mu^2 N_{xx}^T \sum_m m^3 + 240\pi^3 a^2 B_{11} \sum_m m^2 w_{0m} \sum_n n^2 w_{0n} - 480\pi^3 a^2 B_{11} \sum_m m^3 w_{0m}^2 - \\
 &64\pi^3 B_{11} \sum_m u_{0m} + 60\pi^5 \mu^2 B_{11} \sum_m w_{0m} \sum_n w_{0n} - 480\pi^4 a N_{xx}^T \sum_m m \sum_n n - 480\pi^3 a^2 \mu^2 N_{xx}^T + 480\pi^4 a N_{xx}^T \sum_m m + \\
 &7680\pi^3 a^2 D_{11} \sum_m m^2 \sum_n n^2 - 15360\pi^3 a^2 D_{11} \sum_m m \sum_n n \sum_p p + 11520\pi^3 a^2 D_{11} \sum_m m \sum_n n - 3840\pi^3 a^2 D_{11} \sum_m m + \\
 &15\pi^3 a^2 B_{11} \sum_m w_{0m} \sum_n w_{0n} - 120\pi^4 a N_{xx}^T + 480\pi^3 a^2 D_{11} - 4096\pi^3 a \mu^2 B_{11} \sum_m m^4 u_{0m} + 8192\pi^3 a \mu^2 B_{11} \sum_m m^3 u_{0m} - \\
 &6144\pi^3 a \mu^2 B_{11} \sum_m m^2 u_{0m} + 2048\pi^3 a \mu^2 B_{11} \sum_m m u_{0m} - 256\pi^3 a \mu^2 B_{11} \sum_m u_{0m} - 256\pi^3 a B_{11} \sum_m m^2 u_{0m} + 256\pi^3 a B_{11} \sum_m m u_{0m} = 0
 \end{aligned} \tag{A1}$$

Appendix B: Vibration equation

The algebraic equation arising from the Galerkin integration (Eq. (18)) for the vibration case is:

$$\begin{aligned}
 &120\pi^3 a B_{11} \sum_m m^3 u_m - 180\pi^3 a B_{11} \sum_m m^2 u_m + 15\pi^3 a I_0 \omega^2 \sum_m u_m + 90\pi^3 a B_{11} \sum_m m u_m + 15\pi^3 a I_0 \mu^2 \omega^2 \sum_m u_m - \\
 &30\pi^3 a I_0 \omega^2 \sum_m m u_m - 15\pi^3 a B_{11} \sum_m u_m + 32\pi^3 B_{11} \sum_m w_{0m} \sum_n w_n - 256\pi^3 B_{11} \sum_m m \sum_n n \sum_p p \sum_q w_{0q} \sum_r w_r + \\
 &384\pi^3 B_{11} \sum_m m w_{0m} \sum_n n w_n - 192\pi^3 B_{11} \sum_m m \sum_n w_{0n} \sum_p w_p - 120\pi^3 a I_0 \mu^2 \omega^2 \sum_m m^3 u_m + 180\pi^3 a I_0 \mu^2 \omega^2 \sum_m m^2 u_m - \\
 &90\pi^3 a I_0 \mu^2 \omega^2 \sum_m m u_m = 0, \\
 &-192\pi^3 a I_0 \omega^2 \sum_m m \sum_n u_n \sum_p w_{0p} - 60\pi^3 a^2 K \sum_m w_m + 2400\pi^5 D_{11} \sum_m m w_m - 240\pi^5 K \mu^2 \sum_m w_m + 7680\pi^5 D_{11} \sum_m m^5 w_m - \\
 &19200\pi^5 D_{11} \sum_m m^4 w_m + 19200\pi^5 D_{11} \sum_m m^3 w_m - 9600\pi^5 D_{11} \sum_m m^2 w_m + 96\pi^3 a I_0 \omega^2 \sum_m u_m \sum_n w_{0n} - \\
 &480\pi^3 a^2 I_0 \mu^2 \omega^2 \sum_m m^3 w_m + 720\pi^3 a^2 I_0 \mu^2 \omega^2 \sum_m m^2 w_m - 360\pi^3 a^2 I_0 \mu^2 \omega^2 \sum_m m w_m - \\
 &4352\pi^3 a I_0 \mu^2 \omega^2 \sum_m m \sum_n n \sum_p p \sum_q u_q \sum_r w_{0r} + 6528\pi^3 a I_0 \mu^2 \omega^2 \sum_m m u_m \sum_n n w_{0n} - 3264\pi^3 a I_0 \mu^2 \omega^2 \sum_m m \sum_n u_n \sum_p w_{0p} + \\
 &544\pi^3 a I_0 \mu^2 \omega^2 \sum_m u_m \sum_n w_{0n} - 240\pi^5 D_{11} \sum_m w_m + 60\pi^3 a^2 I_0 \mu^2 \omega^2 \sum_m w_m - 480\pi^3 a^2 I_2 \omega^2 \sum_m m^3 w_m + \\
 &720\pi^3 a^2 I_2 \omega^2 \sum_m m^2 w_m - 90\pi^4 a I_0 \omega^2 \sum_m m w_m - 360\pi^3 a^2 I_2 \omega^2 \sum_m m w_m - 19200\pi^5 K \mu^2 \sum_m m^4 w_m + 19200\pi^5 K \mu^2 \sum_m m^3 w_m - \\
 &9600\pi^5 K \mu^2 \sum_m m^2 w_m + 2400\pi^5 K \mu^2 \sum_m m w_m + 7680\pi^5 K \mu^2 \sum_m m^5 w_m + 60\pi^3 a^2 I_2 \omega^2 \sum_m w_m + 480\pi^3 a^2 K \sum_m m^3 w_m - \\
 &720\pi^3 a^2 K \sum_m m^2 w_m + 360\pi^3 a^2 K \sum_m m w_m + 45\pi^4 a I_0 \omega^2 \sum_m w_m + 240\pi^5 I_2 \mu^2 \omega^2 \sum_m w_m - 19200\pi^5 I_2 \mu^2 \omega^2 \sum_m m^3 w_m + \\
 &9600\pi^5 I_2 \mu^2 \omega^2 \sum_m m^2 w_m - 2400\pi^5 I_2 \mu^2 \omega^2 \sum_m m w_m - 7680\pi^5 I_2 \mu^2 \omega^2 \sum_m m^5 w_m + 19200\pi^5 I_2 \mu^2 \omega^2 \sum_m m^4 w_m = 0
 \end{aligned} \tag{B1}$$

Nomenclature

a	length of graphene nanoribbon	j	degree of freedom in x and z directions
E_y	effective Young's moduli	M_y	moment resultants
\bar{E}_y	transformed elastic constants	M^T	thermal moment
I_0, I_2	mass moment of inertias	N_y	in-plane stress resultants
		N^T	thermal force

P	lateral load
u	displacement component due to vibration in x direction
u_0	displacement of middle surface for postbuckled state in x direction
U	total displacements in x direction
w	displacement component due to vibration in z direction
w_0	displacement of middle surface for postbuckled state in z direction
W	total displacements in z direction
α_1	thermal expansion coefficient in x direction
α_2	thermal expansion coefficient in y direction
ε_{xx}^0	nonlinear normal strain component in the plate middle surface
μ	nonlocal parameter
σ'	local stress tensor
σ^{nl}	nonlocal stress tensor

References

- [1] B.L. Dasari, J.M. Nouri, D. Brabazon, S. Naher, Graphene and derivatives - Synthesis techniques, properties and their energy applications, *Energy*, 140 (2017) 766-778.
- [2] R. Saito, G. Dresselhaus, M.S. Dresselhaus, *Physical Properties of Carbon Nanotubes*, Imperial College Press, 1998.
- [3] D. Sen, K.S. Novoselov, P.M. Reis, M.J. Buehler, Tearing Graphene Sheets From Adhesive Substrates Produces Tapered Nanoribbons, *Small*, 6(10) (2010) 1108-1116.
- [4] F. Scarpa, R. Chowdhury, e.a. K. Kam, Dynamics of mechanical waves in periodic graphene nanoribbon assemblies, *Nanoscale Res. Lett.*, 6(430) (2011).
- [5] M. Neek-Amal, F.M. Peeters, Graphene nanoribbons subjected to axial stress, *PHYSICAL REVIEW B*, 82(085432) (2010).
- [6] Y.T. Beni, Size-dependent analysis of piezoelectric nanobeams including electro-mechanical coupling, *Mechanics Research Communications*, 75 (2016) 67-80.
- [7] G.A. Varzandian, S. Ziaee, Analytical Solution of Non-Linear Free Vibration of Thin Rectangular Nano Plates with Various Boundary Conditions Based on Non-Local Theory, *Amirkabir Journal of Mechanical Engineering*, 48(4) (2017) 331-346.
- [8] Y. Tang, Y. Liu, D. Zhao, Wave dispersion in viscoelastic single-walled carbon nanotubes based on the nonlocal strain gradient Timoshenko beam model, *Physica E: Low-dimensional Systems and Nanostructures*, 87 (2017) 301-307.
- [9] Y. Zhen, L. Zhou, Wave propagation in fluid-conveying viscoelastic carbon nanotubes under longitudinal magnetic field with thermal and surface effect via nonlocal strain gradient theory, *Modern Physics Letters B*, 31(8) (2017) 1750069 (16 pages).
- [10] Y.T. Beni, Size-dependent electromechanical bending, buckling, and free vibration analysis of functionally graded piezoelectric nanobeams, *Journal of intelligent material systems and structures*, 27(16) (2016) 2199-2215.
- [11] A.C. Eringen, *Nonlocal Continuum Field Theories*, Springer, New York, 2002.
- [12] A.C. Eringen, On differential equations of nonlocal elasticity and solutions of screw dislocation and surface waves, *J. Appl. Phys.*, 54 (1983) 4703-4710.
- [13] S.C. Pradhan, J.K. Phadikar, Nonlocal elasticity theory for vibration of nanoplates, *J. Sound Vib.*, 325 (2009) 206-223.
- [14] R. Nazemnezhad, Nonlocal Timoshenko beam model for considering shear effect of van der Waals interactions on free vibration of multilayer graphene nanoribbons, *Composite Structures*, 133 (2015) 522-528.
- [15] J.-X.S. et al., Nonlocal vibration of embedded double-layer graphene nanoribbons in in-phase and anti-phase modes, *Physica E.*, 44 (2012) 1136-1141.
- [16] T. Ragab, J. McDonald, C. Basaran, Aspect ratio effect on shear modulus and ultimate shear strength of graphene nanoribbons, *Diamond & Related Materials*, 74 (2017) 9-15.
- [17] K. Cai, L. Liu, J. Shi, Q.H. Qin, Winding a nanotube from black phosphorus nanoribbon onto a CNT at low temperature: A molecular dynamics study, *Materials Design*, 121 (2017) 406-413.
- [18] M. López-Suárez, G. Abadal, L. Gammaitoni, R. Rurali, Noise energy harvesting in buckled BN nanoribbons from molecular dynamics, *Nano Energy*, 15 (2015) 329-334.
- [19] A. Farajpour, M. Danesh, M. Mohammadi, Buckling analysis of variable thickness nanoplates using nonlocal continuum mechanics, *Physica E.*, 44 (2011) 719-727.
- [20] E. Ventsel, T. Krauthammer, *Thin Plates and Shells: Theory, Analysis and Applications*, Marcell Dekker Inc., 2001.
- [21] S.K. Georgantzinos, G.I. Giannopoulos, N.K. Anifantis, Thermoelastic Analysis of Graphene-Based Nanomaterials, *Journal of Computations & Modelling*, 7(1) (2017) 1-14.
- [22] S. Narendar, S. Gopalakrishnan, Temperature effects on wave propagation in nanoplates, *Composites: Part B*, 43 (2012) 1275-1281.
- [23] Y.Z. Wang, F.M. Li, K. Kishimoto, Thermal effects on vibration properties of double-layered nanoplates at small scales, *Composites: Part B*, 42(5) (2011) 1311-1317.
- [24] K.-S. Na, J.-H. Kim, Thermal postbuckling investigations of functionally graded plates using 3-D finite element method, *Finite Elements in Analysis and Design*, 42 (2006) 749-756.
- [25] L. Shen, H.S. Shen, C.L. Zhang, Nonlocal plate model for nonlinear vibration of single layer graphene sheets in thermal environments, *Comput. Mater. Sci.*, 48 (2010) 680-685.
- [26] H.-S. Shen, Y.-M. Xu, C.-L. Zhang, Prediction of nonlinear vibration of bilayer graphene sheets in thermal

- environments via molecular dynamics simulations and nonlocal elasticity, *Comput. Methods Appl. Mech. Engrg.*, 267 (2013) 458-470.
- [27] N. Yamaki, M. Chiba, Nonlinear vibrations of a clamped rectangular plate with initial deflection and initial edge displacement part I: theory, *Thin-Walled Struct.*, 1 (1983) 3-29.
- [28] J.K. Paik, K. Anil, T. amballi, B.J. Kim, Large deflection orthotropic plate approach to develop ultimate strength formulations for stiffened panels under combined biaxial compression/tension and lateral pressure, *Thin-Walled Structures*, 39 (2001) 215-246.
- [29] A.H. Nayfeh, S.A. Emam, Exact solution and stability of postbuckling configurations of beams, *Nonlinear Dynamics*, 54 (2008) 395-408.
- [30] V. Refaiejad, O. Rahmani, S.A.H. Hosseini, An analytical solution for bending, buckling, and free vibration of FG nanobeam lying on Winkler-Pasternak elastic foundation using different nonlocal higher order shear deformation beam theories, *Scientia Iranica F*, 24(3) (2017) 1635-1653.
- [31] A. Norouzzadeh, R. Ansari, H. Rouhi, Isogeometric vibration analysis of small-scale Timoshenko beams based on the most comprehensive size-dependent theory, *Scientia Iranica F*, 25(3) (2018) 1864-1878.
- [32] H. Farokhi, H. Mergen, G.M. Amabili, Nonlinear resonant behavior of microbeams over the buckled state, *Appl. Phys. A.*, 113 (2013) 297-307.
- [33] J.N. Reddy, *Theory and Analysis of Elastic plates and Shells*: 2nd Edition, Taylor & Francis Group, 2007.
- [34] M.T. et.al., Graphene and graphite nanoribbons: Morphology, properties, synthesis, defects and applications, *nano today*, 5 (2010) 351-372.
- [35] M.O. Valappil, V.K. Pillai, S. Alwarappan, Spotlighting graphene quantum dots and beyond: Synthesis, properties and sensing applications, *Applied Materials Today*, 9 (2017) 350-371.
- [36] R. Ansari, S. Sahmani, B. Arash, Nonlocal plate model for free vibrations of single-layered graphene sheets, *Physics Letters A*, 375 (2010) 53-62.
- [37] S.J. Stuart, A.B. Tutein, J.A. Harrison, A reactive potential for hydrocarbons with intermolecular interactions, *Journal of Chemical Physics*, 112 (2000) 6472-6486.
- [38] T.P. Chang, J.Y. Liang, Vibration of Postbuckled Delaminated Beam-Plates, *Int .J. Solids Structures*, 35(12) (1998) 1199-1217.

